© 2018. Published by The Company of Biologists Ltd | Journal of Cell Science (2018) 131, jcs208397. doi:10.1242/jcs.208397

RESEARCH ARTICLE

Phosphorylation of ARHGAP19 by CDK1 and ROCK regulates its subcellular localization and function during mitosis

Claire Marceaux, Dominique Petit, Jacques Bertoglio* and Muriel D. David*

ABSTRACT

ARHGAP19 is a hematopoietic-specific Rho GTPase-activating protein (RhoGAP) that acts through the RhoA/ROCK pathway to critically regulate cell elongation and cytokinesis during lymphocyte mitosis. We report here that, during mitosis progression, ARHGAP19 is sequentially phosphorylated by the RhoA-activated kinases ROCK1 and ROCK2 (hereafter ROCK) on serine residue 422, and by CDK1 on threonine residues 404 and 476. The phosphorylation of ARHGAP19 by ROCK occurs before mitosis onset and generates a binding site for 14-3-3 family proteins. ARHGAP19 is then phosphorylated by CDK1 in prometaphase. The docking of 14-3-3 proteins to phosphorylated S422 protects ARHGAP19 from dephosphorylation of the threonine sites and prevents ARHGAP19 from relocating to the plasma membrane during prophase and metaphase, thus allowing RhoA to become activated. Disruption of these phosphorylation sites results in premature localization of ARHGAP19 at the cell membrane and in its enrichment to the equatorial cortex in anaphase leading to cytokinesis failure and cell multinucleation.

KEY WORDS: ARHGAP19, CDK1, Mitosis, ROCK, Rho GTPase

INTRODUCTION

Rho GTPases are small G proteins involved in a number of signaling pathways that control cell adhesion, migration and cytokinesis (Chircop, 2014; Hall, 2012). Through their ability to bind guanine nucleotide di- or tri-phosphate, GTPases act as molecular switches alternating between an inactive and active state, respectively. Signaling pathway activity is regulated by guanine exchange factors (GEFs) that facilitate the nucleotide exchange from GDP to GTP, and GTPase-activating proteins (GAPs) that catalyze GTP hydrolysis to GDP, resulting in signaling pathway activation and deactivation, respectively. Small GTPases of the Rho family play key regulatory roles during mammalian cell division. In particular, RhoA regulates cortical rigidity during cell rounding and constriction of the actomyosin contractile ring during cytokinesis (Kamijo et al., 2006; Maddox and Burridge, 2003). The activity of Rho GTPases must be tightly regulated to ensure that the various steps of the cell division process occur in a coordinated manner. Previous studies on Rho GTPase regulation during mitosis have underlined the importance of three GEFs, Ect2 (Tatsumoto et al., 1999), GEF-H1 (also known as ARHGEF2) (Birkenfeld et al., 2007) and MyoGEF (also known as PLEKHG6) (Wu et al., 2006) and two GAPs, RacGAP1 (also known as MgcRacGAP) and p190A RhoGAP (also known as ARHGAP35) (Hirose et al., 2001; Su et al., 2003). Recently ARHGAP11A, described as an M-phase GAP, was shown to control the zone of active RhoA in mitotic HeLa cells (Zanin et al., 2013). We have previously shown that the novel hematopoietic cell-specific RhoGAP ARHGAP19 is involved in cell shape changes during lymphocyte mitosis by regulating RhoA activity and subsequent ROCK-mediated phosphorylation of myosin and vimentin (David et al., 2014).

Proteins that are active during cell cycle progression, including Rho-GEFs and -GAPs are tightly regulated during cell division (David et al., 2012). Expression levels of some of the Rho GTPase regulators involved in mitosis control (e.g. Ect2, RacGAP1 or ARHGAP19) fluctuate during the cell cycle and reach their highest level in G2/M (David et al., 2014; Liot et al., 2011; Seguin et al., 2009). Another shared mode of regulation of these proteins is through phosphorylation. Such post-translational modifications often control their ability to interact with other proteins, and thereby affect their subcellular localization. In addition there are examples where phosphorylation directly regulates the activity of a GEF or a GAP by modifying their conformation (Hara et al., 2006; Tripathi et al., 2014). In our previous study on the role of ARHGAP19 in cytokinesis control, we gathered evidence that ARHGAP19 must be subject to post-translational regulations. First, while overexpression of ARHGAP19 delayed cytokinesis onset, it did not impact on the velocity of cleavage furrow ingression, suggesting that ARHGAP19 action was restricted to the early mitosis time window. Second, we noted that localization of ARHGAP19 during mitosis progression was highly dynamic, shuttling between the cytosol, the cell cortex and the nucleus of daughter cells. These observations suggested that one or several mitotic kinases may regulate the subcellular localization of ARHGAP19. Among the numerous kinases that are at play during mitosis, CDK1 is believed to be one of the main coordinators ensuring that cytokinesis does not occur before chromosome segregation (Lindon, 2008). In this paper, we show that ARHGAP19 is phosphorylated by CDK1 on two residues, T404 and T476 located in the C-terminal region of the protein. Furthermore, ARHGAP19 is phosphorylated on S422 by the Rho effector kinases proteins ROCK1 and ROCK2 (hereafter ROCK) thus generating a binding site for 14-3-3 proteins.

We investigated whether these post-translational modifications have an influence on the function or localization of the ARHGAP19 protein during mitosis. Results from microscopy imaging experiments indicated that protein phosphorylation has an impact on its localization, as we observed that the non-phosphorylated mutant forms of ARHGAP19 are recruited at the cell cortex as soon as the prophase step, while wild-type (WT) ARHGAP19 is only recruited at the metaphase to anaphase transition. Cell cortex localization of the non-phosphorylated mutant forms of

Inserm U749 and Inserm U1170, Gustave Roussy, 94805 Villejuif, France.

*Authors for correspondence (jacques.bertoglio@gustaveroussy.fr; muriel.david@gustaveroussy.fr)

C.M., 0000-0002-9107-8772; D.P., 0000-0002-7388-1668; J.B., 0000-0002-9834-376X; M.D.D., 0000-0003-1392-2701

Received 12 July 2017; Accepted 24 January 2018

Journal of Cell Science (2018) 131, jcs208397. doi:10.1242/jcs.208397

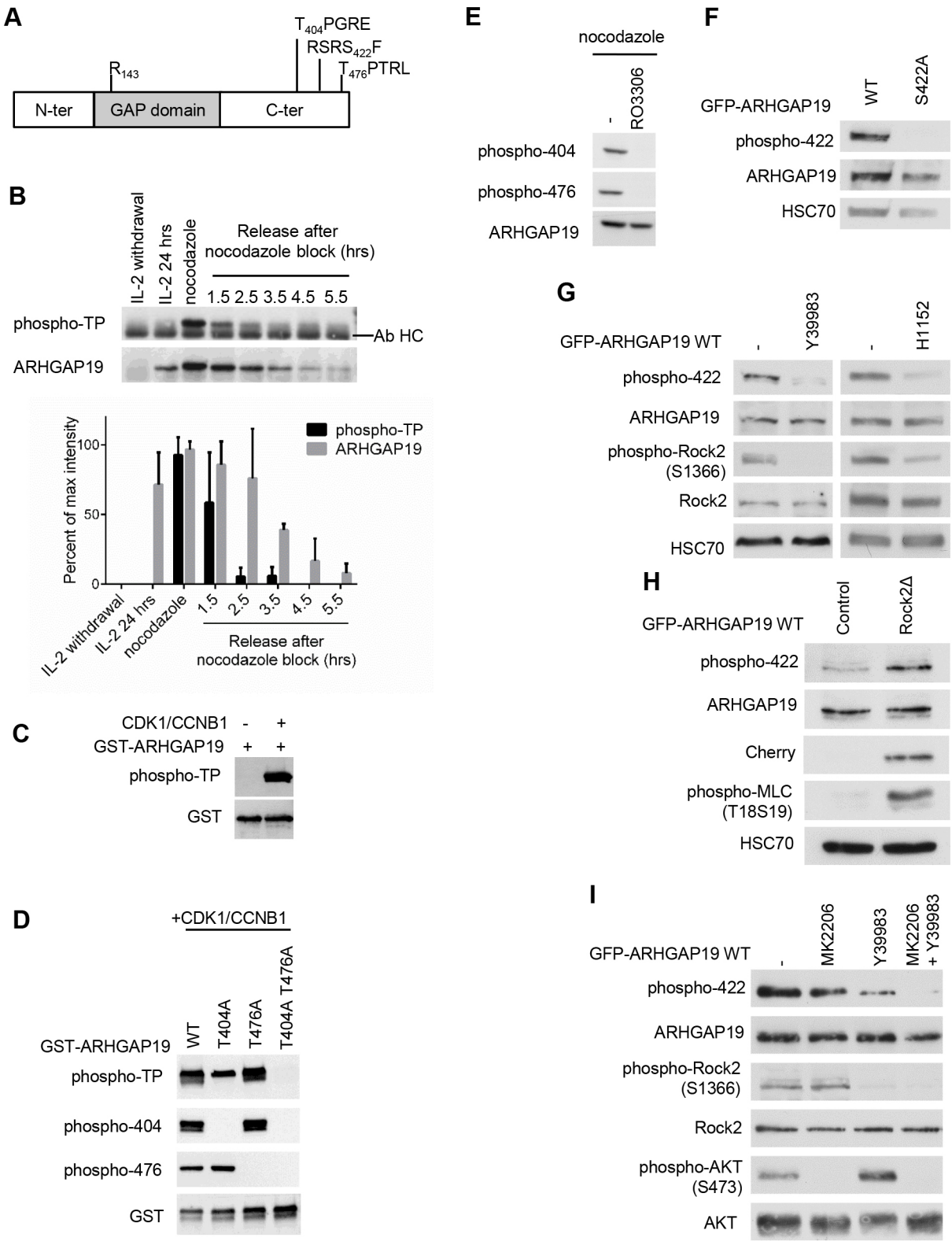

Fig. 1. See next page for legend.

ARHGAP19 at later stages of mitosis was also more pronounced than that of the WT form. Finally, ARHGAP19 phosphorylation appeared to be essential during cell division. Mutation of either the CDK1 or ROCK phosphorylation sites resulted in cytokinesis failure and cell multinucleation.

RESULTS

ARHGAP19 is phosphorylated by CDK1 in early mitosis

CDK1 phosphorylates its substrates on threonine or serine residues present in TP-x-R or SP-x-R motifs, respectively. Analysis of the protein sequence of ARHGAP19 revealed the presence of two

Journal of Cell Science

Journal of Cell Science (2018) 131, jcs208397. doi:10.1242/jcs.208397

Fig. 1. ARHGAP19 is a substrate of CDK1, ROCK and AKT. (A) The CDK1 and ROCK/AKT phosphorylation consensus motifs (S/T-P-x-R/K, R/K-x-x-S/T-x and R-x-R-x-x-S/T-x) are located in the C-terminal region of ARHGAP19 at positions 404, 476 and 422, outside the GAP domain containing the catalytic arginine, R143. (B) IL-2-dependent Kit225 cells were synchronized in G1 by factor deprivation, then stimulated to re-enter the cell cycle by adding back IL-2 for 24 h. Where indicated, cells were blocked in prometaphase by treatment with nocodazole, washed and cultured for up to 5.5 h. Phosphorylation of ARHGAP19 is revealed by an anti-phospho-TP antibody, and the signal rapidly decreases upon removal of nocodazole. As shown previously, endogenous ARHGAP19 levels are cell cycle regulated and reach a maximum in mitosis. The bar graph represents intensities of the phospho-TP and ARHGAP19 signals as mean±s.d. from three independent experiments, expressed as percentages of the maximal signal intensity obtained in each experiment. Ab HC, heavy chain of the anti-ARHGAP19 antibodies used for immunoprecipitation. (C,D) *In vitro* kinase assays. GST–ARHGAP19 in its WT form, or with residues T404 and T476 mutated into non phosphorylatable alanine residues, were incubated in the presence of recombinant CDK1–CCNB1. Western blots were performed using the anti-phospho-TP antibody, and antibodies specifically recognizing the phosphorylated forms of residues T404 and T476. (E) WT ARHGAP19-expressing cells were arrested in prometaphase by treatment with nocodazole and were then incubated with the RO3306 CDK1 inhibitor. Western blotting using the anti-phospho-404 and anti-phospho-476 antibodies indicated that CDK1 inhibition abrogates these phosphorylation events. (F) Specificity of the anti-phospho-422 antibody. WT GFP–ARHGAP19 but not S422A GFP–ARHGAP19 is recognized by this antibody in nocodazole-arrested Kit225 cells. (G) Inhibition of ROCK abolishes the phosphorylation of ARHGAP19 on S422. WT GFP–ARHGAP19-expressing Kit225 cells were synchronized by treatment with nocodazole and incubated in the presence or the absence of the Y39983 or the H1152 ROCK inhibitory compounds. The samples were analyzed by western blotting using anti-phospho-422, anti-ARHGAP19, anti-phospho-ROCK2 and anti-ROCK2 antibodies. HSC70 levels were assessed to control for equal protein loading. (H) ROCK activation leads to an increase in phospho-S422. WT GFP–ARHGAP19-expressing Kit225 cells were transfected with vectors encoding mCherry or mCherry–ROCK2Δ and synchronized by treatment with nocodazole. The samples were analyzed by western blotting using anti-phospho-422, anti-ARHGAP19, anti-Cherry and anti-phospho-MLC antibodies. (I) Inhibition of both ROCK (using Y39983) and AKT (using MK2206) is necessary to abolish the phosphorylation of WT GFP–ARHGAP19 on S422 in nocodazole-synchronized Jurkat cells.

potential phosphorylation sites for CDK1, namely the threonine residues at positions 404 and 476 (Fig. 1A). To assess whether ARHGAP19 is phosphorylated on one or both of these TP-x-R motifs, endogenous ARHGAP19 was immunoprecipitated from Kit225 lymphocytes synchronized in G1, S-G2, prometaphase or later mitotic stages. As shown in Fig. 1B, ARHGAP19 from nocodazole-treated prometaphasic cells is recognized by an anti-phospho-TP-motif antibody. The level of ARHGAP19 phosphorylation on TP motifs decreased upon removal of the synchronizing agent, which allowed cells to resume progression in mitosis. Like Ect2 and MgcRacGAP (Liot et al., 2011; Seguin et al., 2009), ARHGAP19 becomes degraded when cells enter the G1 phase of the next cycle. However, after cell release from the nocodazole-induced block in prometaphase, the phospho-TP signal decreased at a higher rate than that of ARHGAP19, suggesting that there is active dephosphorylation of ARHGAP19 by one or several phosphatases. Given that both T404 and T476 of ARHGAP19 are in motifs fitting the consensus of sites subject to CDK1-mediated phosphorylation, we tested whether active CDK1 can phosphorylate ARHGAP19. In an *in vitro* kinase assay, we found that GST–ARHGAP19 could be phosphorylated on TP motifs in the presence of a recombinant CDK1–CCNB1 complex (Fig. 1C). This phosphorylation is abrogated by the double T404A/T476A mutation, but not by the single T404A or T476A mutations (Fig. 1D). To allow further investigation of the phosphorylation events occurring on T404 and T476, we generated antibodies against the corresponding phospho-peptides. The *in vitro* kinase assay described above allowed us to confirm that these antibodies recognize their respective targets specifically (Fig. 1D).

To confirm the role of CDK1 on the T404/T476 phosphorylation, Kit225 lymphocytes were synchronized in prometaphase by performing a 16 h nocodazole treatment (40 ng/ml) with the RO3306 inhibitory compound (9 µg/ml) being added (or not) for the last 4 h before the cells were processed for western blot analysis. The phospho-T404/T476 signals were abrogated when CDK1 is inhibited by RO3306 treatment (Fig. 1E). This result indicates that T404 and T476 of ARHGAP19 are targeted by the kinase CDK1 in cells.

ARHGAP19 is also phosphorylated by ROCK and AKT

In addition to T404 and T476, mass spectrometric analyses of human ARHGAP19 [our own studies, not shown, and Mertins et al. (2013)] indicate that ARHGAP19 is phosphorylated on multiple residues, including S422, which is conserved among species. S422 lies in an R/K-x-x-S/T-x motif (Fig. 1A) that represents a potential phosphorylation site for the RhoA effector kinase ROCK. To study phosphorylation of ARHGAP19 at this site, we generated anti-phosphopeptide antibodies that specifically recognized the WT but not the S422A mutant form of ARHGAP19 from nocodazole-arrested Kit225 cells (Fig. 1F). To analyze whether ROCK could be responsible for the phosphorylation of ARHGAP19, Kit225 lymphocytes were synchronized in prometaphase using nocodazole and then treated for 90 min with the ROCK inhibitory compounds Y39983 or H1152 (Feng et al., 2016; Ramachandran et al., 2011). As shown in Fig. 1G, inhibition of ROCK, as assessed by the disappearance of the phospho-ROCK2 signal, strongly decreased phosphorylation of ARHGAP19 on S422. To confirm the impact of ROCK on S422 phosphorylation, we generated a plasmid encoding a constitutive active form of ROCK, Cherry–ROCK2Δ, where ROCK2 is devoid of its autoinhibitory domain (Sebbagh et al., 2005). This plasmid was transfected in Kit225 cells that already expressed WT GFP–ARHGAP19. Activity of the ROCK2Δ protein was confirmed by an increase in the phosphorylation of myosin light chain 2 (MLC2, also known as MYL2); a parallel increase in the phosphorylation of ARHGAP19 on S422 was observed (Fig. 1H). Taken together, these results indicated that S422 of ARHGAP19 is a target for ROCK in cells.

The motif surrounding S422 is also a potential phosphorylation site for AKT family proteins (R-x-R-x-x-S/T-x). However, inhibiting AKT in nocodazole-arrested Kit225 using MK2206 did not affect ARHGAP19 phosphorylation on S422. We therefore turned to Jurkat cells, another human T cell line in which AKT is constitutively activated due to PTEN deficiency. In these cells, S422 phosphorylation was partially decreased by treatment with either AKT or the ROCK inhibitors, and the combination of both compounds was required to completely abolish S422 phosphorylation (Fig. 1I). Thus ARHGAP19 is likely phosphorylated by both ROCK and AKT in Jurkat cells.

Timing of ARHGAP19 phosphorylations

In unsynchronized Kit225 cells, as well as in cells synchronized just before entry in mitosis through the use of the RO3306 CDK1 inhibitor, ARHGAP19 appears to only be significantly phosphorylated on S422 and not on T404 or T476 (Fig. 2A). We noted a decrease in the level of S422 phosphorylation in cells treated with RO3306, as compared to what was seen in unsynchronized cells. On the other hand, nocodazole treatment, which allows cells to enter

Journal of Cell Science (2018) 131, jcs208397. doi:10.1242/jcs.208397

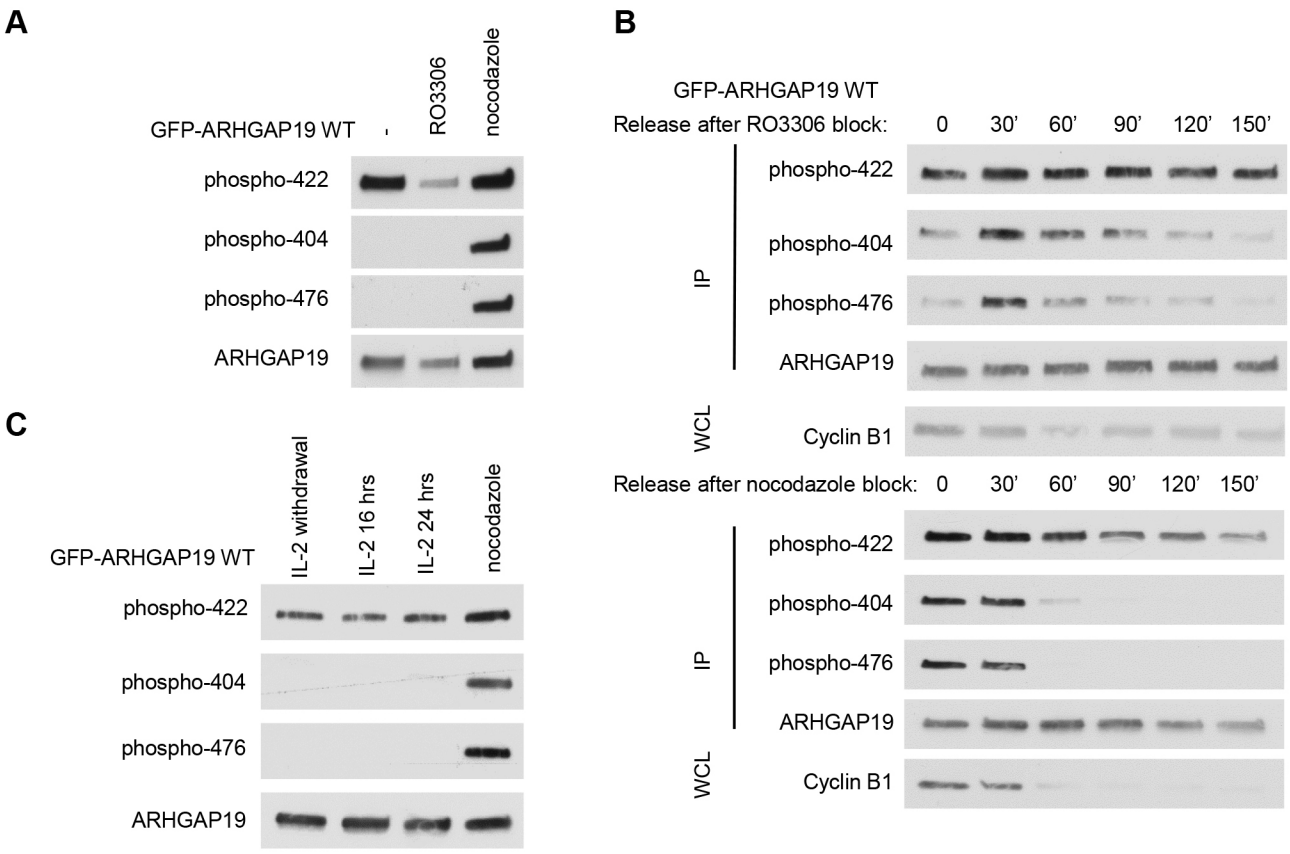

Fig. 2. ARHGAP19 phosphorylation kinetics. (A) WT GFP–ARHGAP19 Kit225 cells were left unsynchronized (–) or synchronized at the G2/M transition by using the CDK1 inhibitor RO3306, or in prometaphase by using nocodazole. In contrast to S422, T404 and T476 are only phosphorylated during mitosis. (B) WT GFP–ARHGAP19 cells were blocked at the G2/M transition or in prometaphase by RO3306 or nocodazole treatment, respectively, and then released into mitosis for the indicated times (minutes). Phosphorylation of S422 is detectable during the entire mitosis while phosphorylation of T404 and T476 residues gradually decreases as cells progress through mitosis (as illustrated by the decrease in cyclin B1 levels, which occurs following the metaphase to anaphase transition). IP, immunoprecipitation; WCL, whole-cell lysates. (C) Kit225 cells were synchronized in G1 by IL-2 deprivation. Addition of IL-2 to the deprived cells then allows them to progress through S phase after 16 h of culture and to reach G2 by 24 h. Prometaphase arrest was achieved by using nocodazole. Phosphorylation of S422 of exogenous GFP–ARHGAP19 is detectable at all phases of the cell cycle while phosphorylation of T404 and T476 is detectable only in mitotic cells.

mitosis but causes arrest in prometaphase, is accompanied by increased levels of phospho-S422, as compared to what was seen in unsynchronized cells, and phosphorylation of ARHGAP19 at positions 404 and 476. Thus, in early mitosis, ARHGAP19 is phosphorylated on all three residues.

We then analyzed more precisely the kinetics of the ARHGAP19 phosphorylations during mitosis. Appearance and disappearance of the phospho-T404/T476 signals in cells synchronized by block and release with either RO3306 or nocodazole are reminiscent of those described for other CDK1 substrates. Indeed, phosphorylation on T404 and T476 increased after mitosis onset, reached a maximum in cells synchronized in prometaphase, and declined thereafter (Fig. 2B). Of note, kinetics of appearance and disappearance of the phosphorylation signals during mitosis progression are similar for T404 and T476 residues, suggesting common regulatory mechanisms. In contrast, phosphorylation on residue S422 decreased slower than phosphorylation on T404 and T476 and was still detectable at the end of mitosis. Furthermore, analyzing the complete cell cycle showed that the S422 of exogenous GFP–ARHGAP19 was phosphorylatable throughout the cell cycle (Fig. 2C) although, as endogenous ARHGAP19 is not expressed in the G1 phase, only phosphorylation from the S-phase and thereafter is of physiological relevance.

Phosphorylation of residues T404/T476 depends on phospho-S422

During the course of this study, we noticed that mutation of a given phosphorylation site (i.e. either S422, T404 or T476) into non-phosphorylatable alanine residues also impacted on the phosphorylation levels of some of the other sites, suggesting that phosphorylation at a given site might influence phosphorylation of other residues. First, not only does RO3306 reduce phosphorylation of S422 (Fig. 2A), but mutation of the T404 and T476 residues into alanine residues does so as well (Fig. 3A). Thus, absence of phosphorylation of T404 and T476 (whether due to cells not being in mitosis, to pharmacological inhibition of CDK1 or to mutation of these residues into alanine) leads to decreased levels of S422 phosphorylation. Second, we observed that, in Kit225 cells, preventing phosphorylation of ARHGAP19 at position 422 either by mutating S422 (Fig. 3A) or by using the ROCK inhibitor (Fig. 3B) correlated with a reduced phosphorylation at positions 404 and 476. These experiments have also been performed in Jurkat cells (Fig. 3C) and led to similar results with the difference that, as described above, inhibition of both AKT and ROCK was required to fully abolish phosphorylation of S422 in Jurkat cells.

Journal of Cell Science (2018) 131, jcs208397. doi:10.1242/jcs.208397

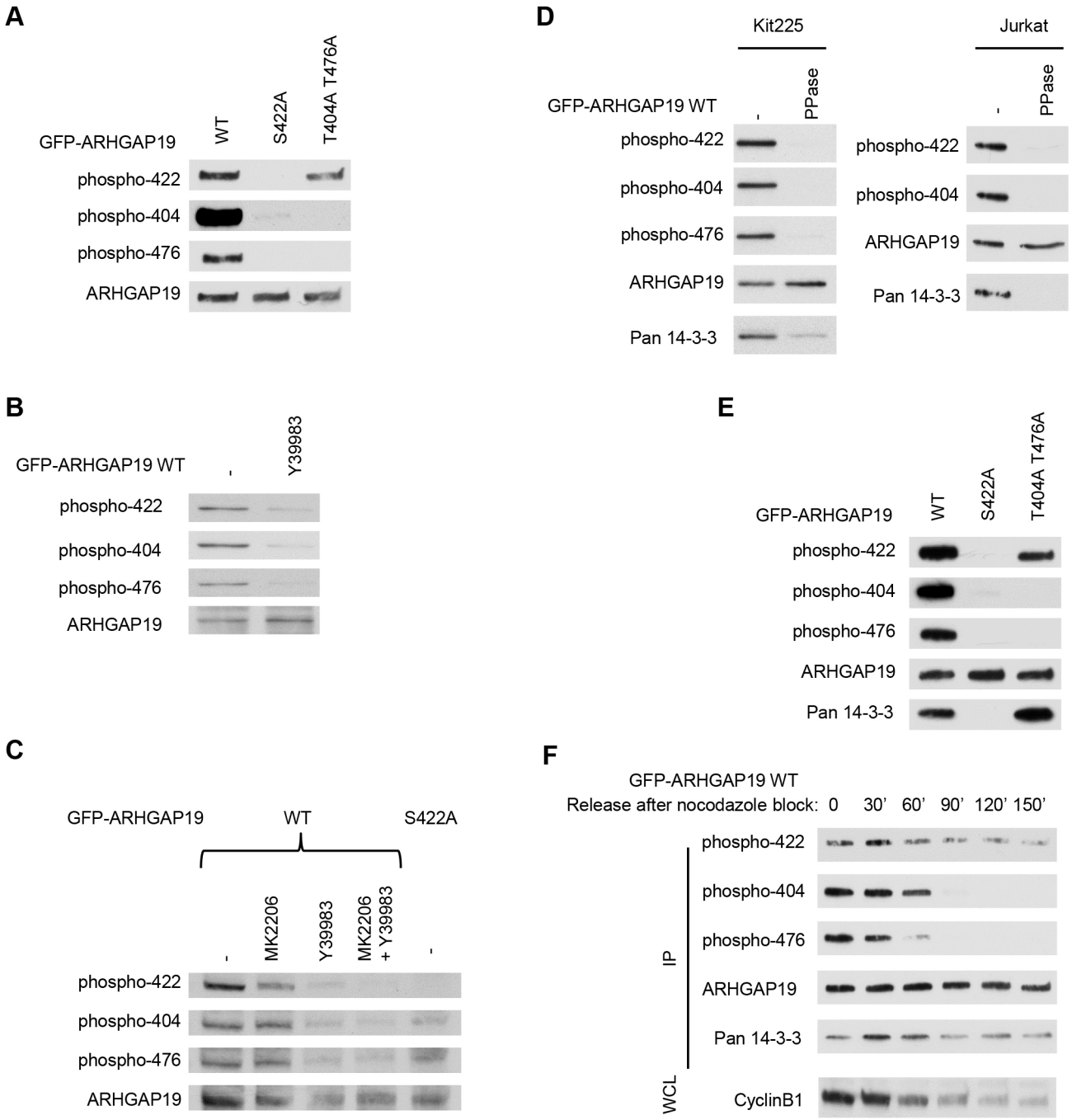

Fig. 3. See next page for legend.

S422-phosphorylated ARHGAP19 interacts with 14-3-3 proteins

Mass spectrometric analysis of ARHGAP19 immune complexes as well as a yeast two-hybrid screen indicated that ARHGAP19 might interact with 14-3-3 family proteins (J.B. and M.D.D., unpublished results). The 14-3-3 protein family is composed of seven proteins that are ubiquitously expressed and bind to phosphoserine and phosphothreonine motifs (Aitken, 1996). 14-3-3 proteins (recognized by a pan-14-3-3 antibody in western blots) are readily detectable in ARHGAP19 immunoprecipitates from nocodazole-treated Kit225 cells (Fig. 3D, left panel) or Jurkat cells (Fig. 3D, right panel). This interaction was abrogated, however, when the immunoprecipitates were dephosphorylated *in vitro* by incubation in the presence of a recombinant PP1 phosphatase. We then analyzed which of the ARHGAP19 phosphoresidues was implicated in this interaction with 14-3-3. 14-3-3 binding was detectable in ARHGAP19 mutated on both T404 and T476 but disappeared with ARHGAP19 S422A (Fig. 3E). Similarly, binding of 14-3-3 to WT ARHGAP19 was detectable in asynchronous cells, or in cells treated with the CDK1 inhibitor RO3306 in which S422 is phosphorylated but T404/T476 are not phosphorylated (data not shown). Thus, binding of 14-3-3 proteins appeared to be mediated by phospho-S422, which indeed lies in a consensus motif for 14-3-3 proteins (RS-x-pS/T-x or R-xxx-pS/T-x) (Fernández-Orth et al., 2017; Yaffe et al., 1997).

Journal of Cell Science

Journal of Cell Science (2018) 131, jcs208397. doi:10.1242/jcs.208397

Fig. 3. Phosphorylation of S422 promotes T404/T476 phosphorylation and mediates interaction of ARHGAP19 with 14-3-3 proteins. (A) Phosphorylation of T404 and T476 disappears when S422 is non-phosphorylatable. Kit225 cells expressing either WT GFP–ARHGAP19 or the S422A or the T404A/T476A GFP–ARHGAP19 mutants were synchronized in prometaphase by using nocodazole. GFP–ARHGAP19 was immunoprecipitated with GFP-Trap®, and western blotting was performed using anti-phospho-422, anti-phospho-404, anti-phospho-476 and anti-ARHGAP19 antibodies. (B) Cell treatment with the ROCK inhibitor decreases the phosphorylation levels of T404 and T476, in addition to that of S422. WT GFP–ARHGAP19-expressing Kit225 cells were synchronized by using nocodazole and cultured for 1.5 h in the absence or the presence of the ROCK inhibitor (Y39983). GFP–ARHGAP19 proteins were analyzed by western blotting in total cell lysates, using the indicated antibodies. (C) In Jurkat cells, phosphorylation levels of T404/T476 drop when S422 phosphorylation is decreased in the presence of kinase inhibitors or when S422 is mutated into a non-phosphorylatable amino acid (S422A). Jurkat cells expressing WT or S422A GFP–ARHGAP19 were synchronized in prometaphase by using nocodazole, and cultured for 1.5 h in the absence or the presence of inhibitors of ROCK (Y39983) or AKT (MK2206). (D) WT ARHGAP19 interacts with 14-3-3 proteins and this interaction is phosphorylation dependent. Kit225 cells (left) or Jurkat cells (right) expressing WT GFP–ARHGAP19 were synchronized in prometaphase by using nocodazole, and GFP–ARHGAP19 proteins were immunoprecipitated with GFP-Trap®. The GFP–ARHGAP19 immunoprecipitates were then treated with recombinant PP1 phosphatase (PPase), or were left untreated. Western blotting was performed with the indicated antibodies. (E,F) Phosphorylation of S422 mediates the interaction of ARHGAP19 with 14-3-3 proteins. (E) Kit225 cells expressing either WT, S422A or T404A/T476A GFP–ARHGAP19 were synchronized in prometaphase. GFP–ARHGAP19 proteins were immunoprecipitated with GFP-Trap®, and western blotting was performed with the indicated antibodies. (F) The interaction with 14-3-3 is detectable throughout all mitosis stages. Kit225 cells expressing WT GFP–ARHGAP19 were synchronized in prometaphase by using nocodazole, and were then washed and released in fresh culture medium for the indicated times. GFP–ARHGAP19 proteins were immunoprecipitated (IP) with GFP-Trap® and western blotting was performed with the indicated antibodies. Western blot analysis of cyclin B1 was performed on whole-cell lysates (WCL).

Furthermore, results shown in Fig. 3F demonstrate that, during mitosis, 14-3-3 proteins bind to ARHGAP19 as long as S422 is phosphorylated.

Binding of 14-3-3 proteins protects ARHGAP19 from dephosphorylation of the T404 and T476 residues

As shown in Fig. 3E, mutation of S422 of ARHGAP19 impedes both the ability of ARHGAP19 to interact with 14-3-3 proteins and the levels of phosphorylation of the T404 and T476 residues, suggesting that both phenomena are linked. Two hypotheses can explain the role of 14-3-3 binding in regulating the T404 and T476 phosphorylations: (1) 14-3-3 proteins could play the role of an adaptor protein and recruit the CDK1 kinase to phosphorylate ARHGAP19, or (2) 14-3-3 proteins could protect ARHGAP19 from dephosphorylation through steric hindrance, limiting access of protein phosphatases to the T404/T476 residues. To test these hypotheses, nocodazole-arrested Kit225 cells expressing WT ARHGAP19 or the S422A mutated form were treated with 100 nM of the serine/theronine phosphatase inhibitor okadaic acid (OA) for 2.5 h. We observed that cell treatment with OA only led to a small increase in phosphorylation of WT ARHGAP19 whereas phosphorylation of both threonine residues was totally rescued in ARHGAP19 S422A cells (Fig. 4A). These results suggest that binding of 14-3-3 to S422, rather than allowing the recruitment of CDK1, may prevent access of an okadaic acid-sensitive phosphatase to phospho-T404/T476.

Phosphorylation of ARHGAP19 prevents its translocation to the cell cortex

A hypothesis that we first investigated was whether phosphorylation of ARHGAP19 modified its GAP activity. To assess ARHGAP19 GAP activity we had to immunoprecipitate the protein from cell lysates. Indeed, *E. coli*-derived recombinant full-length ARHGAP19 is inactive (both as a GST and an MBP fusion protein), even after *in vitro* phosphorylation by a mixture of CDK1 and ROCK (data not shown). In initial experiments, we used cells synchronized with nocodazole or with the CDK1 inhibitor to compare the GAP activity of ARHGAP19 when phosphorylated on T404/T476 or not, respectively. Neither the level of GAP activity towards RhoA nor ARHGAP19 specificity towards RhoA and not Rac or Cdc42 appeared to depend upon its phosphorylation status (Fig. S1A). To further investigate this point, we compared activity of WT ARHGAP19 and ARHGAP19 that had been mutated on all three phosphorylation sites (Fig. S1B) and again found no evidence that phosphorylation might regulate the GAP activity of ARHGAP19.

We next investigated localization of WT, T404A/T476A, S422A or T404A/S422A/T476A in Kit225 cells during mitosis by performing fluorescence microscopy. Following mitosis entry, WT ARHGAP19 was dispersed in the cytoplasm in prophase and metaphase, translocated to the cell cortex in early anaphase, and then concentrated at the cortical region of the ingression cleavage furrow at later stages and until the end of cell division (David et al., 2014). A striking observation is the modification of the localization of the mutated forms (T404A/T476A, S422A or T404A/S422A/T476A) of ARHGAP19 during early mitosis (prophase and metaphase). Indeed, the mutant forms of ARHGAP19 were no longer in the cytoplasm but concentrated at the cell cortex (Fig. 4B,C), suggesting that all three residues contribute to the phenotype. Alternatively, this similarity in the effects of each mutation on ARHGAP19 localization may be the result of the above-described interplay between the phosphorylation status of S422, on one hand, and T404/T476, on the other hand. Thus, phosphorylation of any of these three residues may contribute to the sequestering of ARHGAP19 in the cytoplasm and prevent it from translocating prematurely to the cell cortex. Moreover, quantitative analyses of fluorescence intensities indicated that the recruitment to the cell cortex of the non-phosphorylated mutant forms of ARHGAP19 was also more pronounced than that of the WT form at later stages of mitosis (Fig. 4C).

We have previously reported that silencing ARHGAP19, or expressing its R143A GAP inactive mutant, induced precocious cleavage furrow ingression that, in some cells, leads to failure of cytokinesis and the appearance of binucleated cells (David et al., 2014). To assess whether phosphorylation of ARHGAP19 might have any effect on the outcome of cell division, Kit225 cells were induced to express either WT ARHGAP19 or its mutated forms and were analyzed 48 h later for DNA content by FACS analysis. Cells expressing WT ARHGAP19 had a normal ploidy (between 2N and 4N). In contrast, cells that expressed any of the mutated forms of ARHGAP19 displayed a significant proportion of cells with 8N or even 16N DNA (Fig. 4D). These results demonstrate that the phosphorylations of ARHGAP19, in addition to regulating its subcellular localization, have an impact on cell division.

DISCUSSION

In this study, we report that ARHGAP19 is phosphorylated by the Rho kinase ROCK on S422 and by CDK1 on T404 and T476. ARHGAP19 is localized in the nucleus before mitosis and is phosphorylated on S422 by the Rho kinase ROCK. This

Journal of Cell Science (2018) 131, jcs208397. doi:10.1242/jcs.208397

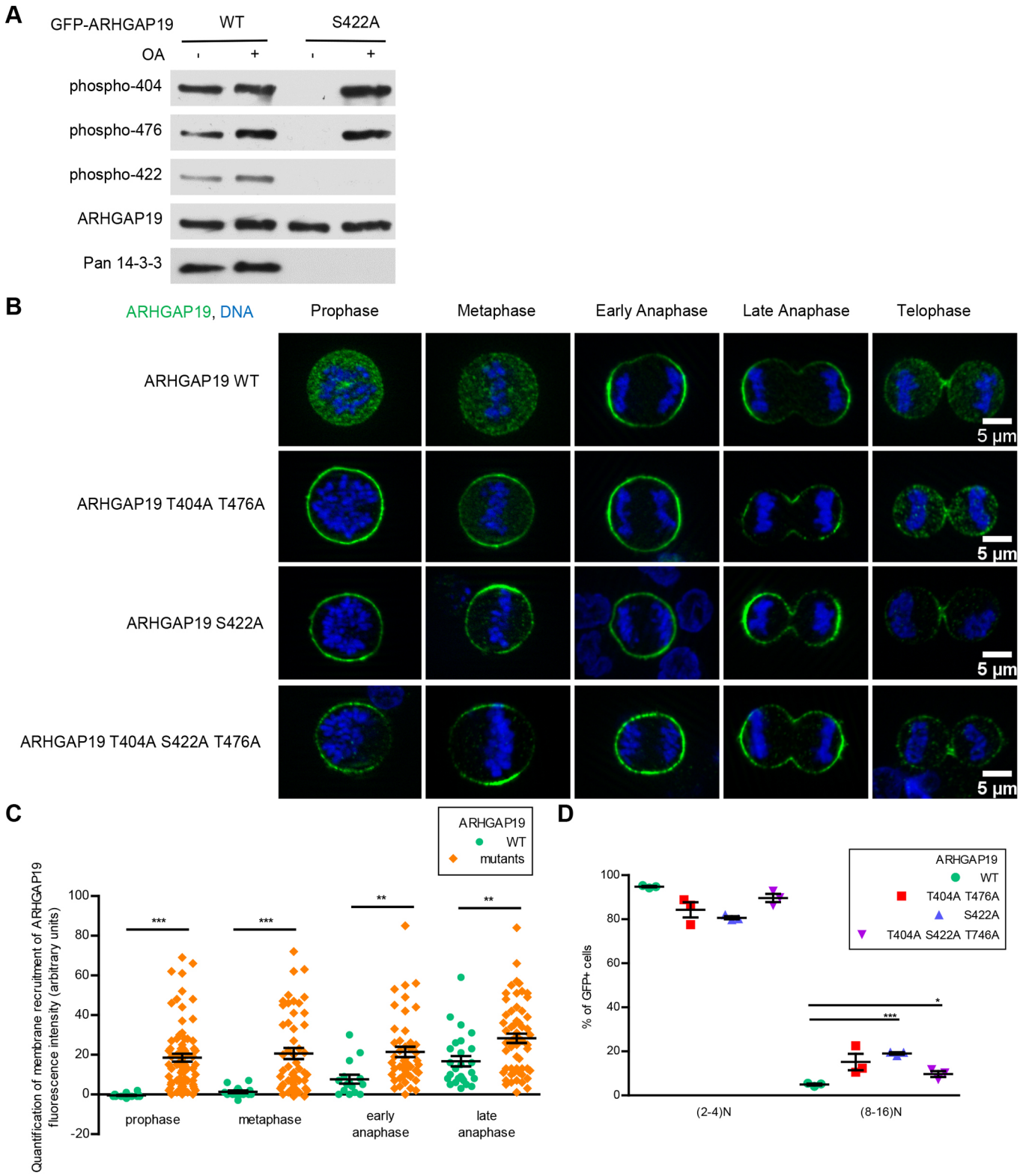

Fig. 4. See next page for legend.

phosphorylation allows the interaction of ARHGAP19 with 14-3-3 proteins. At the beginning of mitosis, the nuclear membrane breaks down and ARHGAP19 moves to the cytoplasm. The kinase CDK1 is then activated, and cytoplasmic CDK1 molecules (Takizawa and Morgan, 2000) phosphorylate ARHGAP19 on the two residues T404 and T476. These phosphorylations persist until CDK1 is inactivated following degradation of cyclin B. Interestingly, phosphorylation on S422 on one hand and on T404/T476 on the other hand appear to influence each other. When ARHGAP19 is not phosphorylated on S422 (e.g. in the S422A mutant), the binding to 14-3-3 proteins is lost

Journal of Cell Science (2018) 131, jcs208397. doi:10.1242/jcs.208397

Fig. 4. Role of phosphorylations of ARHGAP19 and 14-3-3 binding. (A) 14-3-3 binding protects ARHGAP19 from dephosphorylation on T404 and T476. Kit225 cells expressing either WT or S422A GFP–ARHGAP19 were synchronized in prometaphase and treated with OA, a protein phosphatase inhibitor. GFP–ARHGAP19 was immunoprecipitated using GFP-Trap®, and the samples were analyzed by western blotting using the anti-phospho-422, anti-phospho-404, anti-phospho-476, anti-ARHGAP19 and anti-pan-14-3-3 antibodies. (B) Localization of ARHGAP19 during mitosis. Kit225 lymphocytes (expressing the WT, S422A, T404A/T476A or S422A/T404A/T476A forms of ARHGAP19) were fixed with trichloroacetic acid (TCA). Cells were labeled for DNA (Hoechst 33342, blue) and GFP–ARHGAP19 (green) and observed by fluorescence microscopy. Representative pictures are shown. (C) Quantification of ARHGAP19 translocation to the cell cortex during mitosis for cells expressing WT GFP–ARHGAP19 or the S422A, T404A/T476A or the triple T404A/S422A/T476A mutant. Since no significant difference was observed between mutants, results are represented together on the graph under the label 'mutants'. For cells in prophase, fluorescence intensities were measured at random membrane positions. For cells in metaphase or anaphase, fluorescence intensities were measured at the presumptive cleavage furrow or cleavage furrow membranes, respectively. Values corresponding to fluorescence intensities in the cytoplasm were subtracted from that measured at the membrane. Data are expressed as mean±s.e.m. of these calculated values, with $n>10$ for each mitotic stage of each cell population. (D) DNA content analysis. WT and mutant forms of GFP–ARHGAP19 were expressed for 48 h in Kit255 cells. DNA content, assessed through staining with Hoechst 33342, was analyzed by flow cytometry. Results are mean±s.e.m.; $n=3$ for each condition. *$P<0.05$, **$P<0.01$, ***$P<0.0001$ (Student's t-test).

and the phosphorylation of T404 and T476 is decreased. Indeed, our results indicate that the interaction with 14-3-3 proteins protects ARHGAP19 from dephosphorylation by phosphatases, as previously reported for other phosphatase substrates (Gohla and Bokoch, 2002; Hausser et al., 2006). Dependency of the S422 phosphorylation on the status of T404/T476, as observed in RO3306-treated cells or in the T404A/T476A mutant ARHGAP19, is not clearly understood. So far, none of our attempts at investigating the underlying mechanism provided us with any hints to explain it. One hypothesis could be that, because S422 lies in between T404 and T476, the proximity of these three sites might interfere with their respective phosphorylation.

In early mitosis, the mutant ARHGAP19 proteins where S422, T404/T476 or all three residues have been replaced by non-phosphorylatable alanine residues, localize at the membrane and no longer reside in the cytoplasm. Thus, the phosphorylation of these residues prevents ARHGAP19 from interacting with the membrane, possibly due to an increase in the negative charges of the protein or through interaction with 14-3-3.

The precise localization of ARHGAP19 during mitosis progression appears to be crucial for cell division. Indeed, when some of the residues are not phosphorylated, multinucleated cells could be observed by microscopy (data not shown) or through FACS analyses of their DNA content. It has been clearly established that interfering with RhoA activity during mitosis prevents contraction of the actomyosin ring and leads to failure of cytokinesis and multinucleation in various cell types (Kamijo et al., 2006; Yoshizaki et al., 2004). It is therefore likely that the premature membrane localization of non-phosphorylatable ARHGAP19 impedes local RhoA activation and in turn alters and/or delays the cortical contractility that is required for cell shape changes in early mitosis. Indeed, most cells that express ARHGAP19 mutated on these residues do not elongate, a phenomenon that could be directly responsible for delaying chromosome separation and for the subsequent failure of cell division. Moreover, in subsequent steps of mitosis, increased enrichment to the cell equatorial cortex of the mutated forms of ARHGAP19, as compared to the WT form, likely leads to defects in the RhoA-dependent contraction of the cleavage furrow without which cytokinesis cannot occur.

In summary, our data add ARHGAP19 to the list of mitosis related proteins that are substrates of CDK1 and provide evidence for a new regulatory pathway whereby RhoA-activated ROCK phosphorylates ARHGAP19 on S422 to recruit 14-3-3 proteins which, in turn, help to maintain the phosphorylation of residues T404/T476 by CDK1 and impede the ability of ARHGAP19 to translocate prematurely to the cell cortex during mitosis (Fig. 5).

MATERIALS AND METHODS

Cell culture and transfection

Interleukin-2 (IL-2)-dependent human Kit225 lymphocytes and human leukemia Jurkat T cells (ACC 282) were grown and transfected as previously described (David et al., 2014). Stable transfectants were selected in the presence of 2 µg/ml puromycin (for GFP–ARHGAP19 plasmids) or 3.5 µg/ml geneticin (for the Cherry–ROCK2Δ plasmid). To synchronize cells in the G1 phase, lymphocytes were cultured in the absence of IL-2 for 48 h. Cell cycle progression was then resumed by addition of IL-2 for 16 or 24 h, at which time points most cells have reached the S and G2 phases, respectively.

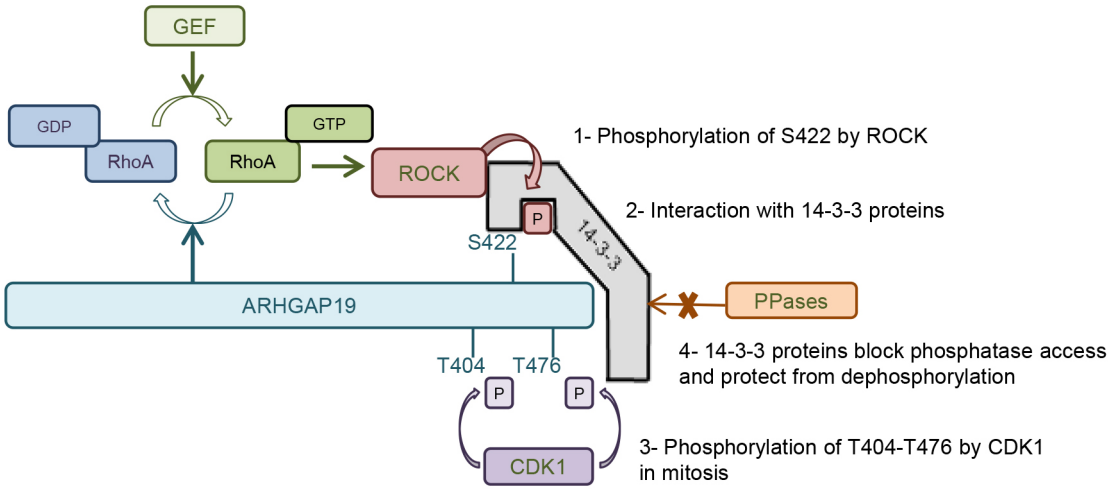

Fig. 5. A schematic model summarizing the regulation of ARHGAP19. Regulatory pathway whereby RhoA-activated ROCK phosphorylates ARHGAP19 on Ser422 (1) to recruit 14-3-3 proteins (2), which, in turn, help maintain the CDK1-mediated phosphorylation of the T404/T476 residues (3) by blocking access of a phosphatase (4) and limiting the ability of ARHGAP19 to translocate to the cell cortex during mitosis.

To enrich the population in prometaphase-blocked cells, 40 ng/ml nocodazole (Sigma-Aldrich, St Louis, MO) was added for 16 h (starting 24 h after IL-2 addition). Where indicated, cells were treated for 20 h with 9 µM RO3306 (Calbiochem, CA) to synchronize them at the end of the G2 phase. Cells were then washed thoroughly and placed in IL-2-containing culture medium to allow progression through mitosis. To inhibit ROCK, cells were treated for 1.5 h with 20 µM Y39983 (Selleckchem, MD) or 10 µM H1152 (Tocris Bioscience, Bio-techne Europe). AKT kinase inhibition was achieved with 1 µM MK2206 (Selleckchem, MD). Cell treatment with 100 nM okadaic acid (#459618, Calbiochem) for 2.5 h was used to inhibit serine/threonine phosphatases.

Plasmids

To generate the mutated forms of ARHGAP19 described in this study, the plasmid encoding inducible GFP–ARHGAP19 (David et al., 2014) was used as a template for site-directed mutagenesis (QuikChange II XL Site-Directed Mutagenesis Kit from Stratagene, La Jolla, CA) together with appropriate primers bearing threonine to alanine, or serine to alanine codon changes. To generate the plasmid allowing inducible Cherry–ROCK2Δ expression, the ROCK2Δ DNA sequence (Sebbagh et al., 2005) was inserted in frame in the pmCherry-C1 plasmid (Clontech). The CMV promoter was then replaced by an AseI-SacI sequence containing the six tetracyclin responsive elements and the minimal CMV promoter from pTRIPZ (Open Biosystem).

In vitro assays

For kinase assays, 2 µg of GST–ARHGAP19 recombinant proteins (David et al., 2014) was affinity purified on glutathione–Sepharose beads (GE Healthcare, Uppsala, Sweden) and incubated with 0.16 U active Cdk1–CyclinB (Millipore, Billerica, MA) in 40 µl kinase buffer (20 mM MOPS pH 7.2, 20 mM β-glycerophosphate, 0.1 mM Na_3VO_4, 20 mM $MgCl_2$, 2 mM DTT, 50 µM ATP) for 30 min at 30°C. After poly-acrylamide gel electrophoresis and protein transfer onto PVDF membranes, the presence of phosphorylated proteins was assessed using the indicated anti-phospho antibodies.

Dephosphorylation was performed for 30 min at 30°C with 12 U recombinant PP1 phosphatase (P0754S, NEB).

In vitro GAP assay

Doxycyclin-treated GFP–ARHGAP19 Kit225 cells (expressing either the WT or the T404A/S422A/T476A mutant) were synchronized in G2 or prometaphase by treatment with RO3306 (9 µg/ml) or nocodazole (40 ng/ml) for 20 h and 16 h, respectively. GFP–ARHGAP19 was then immunoprecipitated using GFP-Trap® beads (Chromotek GMBH, Planegg-Martinsried, Germany) and incubated in the presence of recombinant GTPases (His-tagged RhoA, Rac1 or Cdc42) and GTP, in an optimized buffer provided by Cytoskeleton (Denver, CO). The inorganic phosphate release resulting from the GTPase-dependent hydrolysis of GTP is then measured through a colorimetric assay, according to the manufacturer's instructions. Mock GFP-Trap® immunoprecipitates from cells that do not express GFP–ARHGAP19, which were processed in parallel, were used to assess intrinsic GTP hydrolysis in the absence of the GAP. Data are expressed as a ratio of the inorganic phosphate released in ARHGAP19-containing samples over that released in mock GFP-Trap® immunoprecipitate-containing controls.

Antibodies

Rabbit SY1985 anti-ARHGAP19 antibody was produced in-house and used at 1 µg/ml. Rabbit anti-phospho-S422, rabbit anti-phospho-T404 and rabbit antiphospho-T476 antibodies were produced and purified by ProteoGenix (Schiltigheim, France), using phosphorylated peptides as immunogens, and were used at 1 µg/ml. Rabbit anti-Cyclin B1 (1:1000, sc-752), mouse anti-pan 14-3-3 (1:100, sc-1657), goat anti-ROCK2 (1 µg/ml, sc-1851) and mouse anti-HSC70 (1:2000, sc-7298) were from Santa Cruz Biotechnology (Santa Cruz, CA). Rabbit anti-mCherry (1:1000, ab183628) and mouse anti-mCherry (1:1000, ab125096) were from Abcam (Cambridge, UK). Rabbit anti-AKT (1:2000, 9272), rabbit anti-phospho-Thr18/Ser19-MLC2 (1:1000, 3674), mouse anti-phospho-Thr/Pro (1:5000, 9391) were from Cell Signaling Technology (Ipswich, MA). Goat anti-GST antibody (1:1000, GE27-4577-01) was from Pharmacia Biotech (Uppsala, Sweden). Rabbit anti-phospho-Ser473-AKT (1:2000, 05-1003) was from Merck Millipore. Rabbit anti-phospho-Ser1366-ROCK2 (1 µg/ml, GTX-122651) was from GeneTex (Irvine, CA). Horseradish peroxidase (HRP)-conjugated anti-mouse-IgG anti-rabbit-IgG and anti-goat-IgG secondary antibodies were purchased from GE Healthcare (Uppsala, Sweden), Cell Signaling Technology (Ipswich, MA) and Dako (A/S, Denmark), respectively. The secondary antibody used for microscopy, conjugated to Alexa Fluor 488 was from Molecular Probes (Eugene, OR).

Immunoprecipitation and western blotting

For immunoprecipitation of GFP–ARHGAP19, GFP-trap_A (Chromotek) and 1 mg of whole-cell lysates were used as described in David et al. (2014). Poly-acrylamide gel electrophoresis, transfer onto PVDF membranes (GE Healthcare) and western blots were performed according to standard procedures. All western blots shown are representative of at least three independent experiments.

Microscopy on fixed cells

Lymphocytes were fixed (in suspension) for 10 min using a solution of 10% trichloroacetic acid in water at 4°C and then processed as described in David et al. (2014). Images of optical sections were acquired using a Zeiss AxioImager Z1 fluorescence upright microscope (Zeiss, Jena, Germany) equipped with motorized Z drive, apotome and a 63×/1.40 NA oil M27 objective, and the AxioVision Zeiss software. The illumination settings and acquisition parameters used (including the linear mode) were kept constant to allow faithful comparisons of the fluorescence intensities between cells. Images processing (cropping) and quantifications were performed with ImageJ software. Fluorescence data were analyzed using the Prism software and statistical significance was calculated with Student's *t*-test and denoted as $*P<0.05$, $**P<0.01$, $***P<0.0001$. Contrast settings of the representative images shown in Fig. 4B were minimum and maximum adjusted (linear processing) for a better display.

Flow cytometry

For multinucleation assays, GFP–ARHGAP19 expression was induced by 1 µg/ml doxycyclin for 48 h. At 1 h before analysis with the cytometer BD LSRFortessa™, cells were labeled at 37°C with 10 µg/ml of Hoechst 33342 (B2261, Sigma). Fluorescence data from three independent experiments were analyzed using the Prism program and statistical significance was calculated with Student's *t*-test and denoted as $*P<0.05$, $**P<0.01$, $***P<0.0001$.

Acknowledgements

We thank Khadie Kouyate for expert technical assistance. This work has benefited from the facilities and expertise of the Imaging and Cytometry Platform (Yann Lecluse and Philippe Rameau, UMS AMMICa, Gustave Roussy Cancer Campus, Villejuif, France).

Competing interests

The authors declare no competing or financial interests.

Author contributions

Conceptualization: J.B., M.D.D.; Methodology: C.M., D.P. M.D.D.; Validation: C.M., D.P., M.D.D.; Formal analysis: C.M., D.P., M.D.D.; Investigation: C.M., D.P., M.D.D.; Writing - original draft: C.M., D.P., M.D.D.; Writing - review & editing: J.B., M.D.D.; Supervision: J.B., M.D.D.

Funding

This work was supported by institutional grants from Institut National de la Santé et de la Recherche Médicale (INSERM) and, in its early phase, by a grant from Ligue Contre le Cancer (équipe labellisée to J.B.). C.M. was supported by doctoral grants from Ministère de l'Enseignement Supérieur et de la Recherche (MESR) and Ligue Contre le Cancer.

Supplementary information

Supplementary information available online at
http://jcs.biologists.org/lookup/doi/10.1242/jcs.208397.supplemental

References

Aitken, A. (1996). 14-3-3 and its possible role in co-ordinating multiple signalling pathways. *Trends Cell Biol.* **6**, 341-347.

Birkenfeld, J., Nalbant, P., Bohl, B. P., Pertz, O., Hahn, K. M. and Bokoch, G. M. (2007). GEF-H1 modulates localized RhoA activation during cytokinesis under the control of mitotic kinases. *Dev. Cell* **12**, 699-712.

Chircop, M. (2014). Rho GTPases as regulators of mitosis and cytokinesis in mammalian cells. *Small GTPases* **5**, e29770.

David, M., Petit, D. and Bertoglio, J. (2012). Cell cycle regulation of Rho signaling pathways. *Cell Cycle* **11**, 3003-3010.

David, M. D., Petit, D. and Bertoglio, J. (2014). The RhoGAP ARHGAP19 controls cytokinesis and chromosome segregation in T lymphocytes. *J. Cell Sci.* **127**, 400-410.

Feng, Y., LoGrasso, P. V., Defert, O. and Li, R. (2016). Rho Kinase (ROCK) inhibitors and their therapeutic potential. *J. Med. Chem.* **59**, 2269-2300.

Fernández-Orth, J., Ehling, P., Ruck, T., Pankratz, S., Hofmann, M.-S., Landgraf, P., Dieterich, D. C., Smalla, K.-H., Kähne, T., Seebohm, G. et al. (2017). 14-3-3 Proteins regulate K2P 5.1 surface expression on T lymphocytes. *Traffic* **18**, 29-43.

Gohla, A. and Bokoch, G. M. (2002). 14-3-3 regulates actin dynamics by stabilizing phosphorylated cofilin. *Curr. Biol.* **12**, 1704-1710.

Hall, A. (2012). Rho family GTPases. *Biochem. Soc. Trans.* **40**, 1378-1382.

Hara, T., Abe, M., Inoue, H., Yu, L.-R., Veenstra, T. D., Kang, Y. H., Lee, K. S. and Miki, T. (2006). Cytokinesis regulator ECT2 changes its conformation through phosphorylation at Thr-341 in G2/M phase. *Oncogene* **25**, 566-578.

Hausser, A., Link, G., Hoene, M., Russo, C., Selchow, O. and Pfizenmaier, K. (2006). Phospho-specific binding of 14-3-3 proteins to phosphatidylinositol 4-kinase III beta protects from dephosphorylation and stabilizes lipid kinase activity. *J. Cell Sci.* **119**, 3613-3621.

Hirose, K., Kawashima, T., Iwamoto, I., Nosaka, T. and Kitamura, T. (2001). MgcRacGAP is involved in cytokinesis through associating with mitotic spindle and midbody. *J. Biol. Chem.* **276**, 5821-5828.

Kamijo, K., Ohara, N., Abe, M., Uchimura, T., Hosoya, H., Lee, J.-S. and Miki, T. (2006). Dissecting the role of Rho-mediated signaling in contractile ring formation. *Mol. Biol. Cell* **17**, 43-55.

Lindon, C. (2008). Control of mitotic exit and cytokinesis by the APC/C. *Biochem. Soc. Trans.* **36**, 405-410.

Liot, C., Seguin, L., Siret, A., Crouin, C., Schmidt, S. and Bertoglio, J. (2011). APC(cdh1) mediates degradation of the oncogenic Rho-GEF Ect2 after mitosis. *PLoS ONE* **6**, e23676.

Maddox, A. S. and Burridge, K. (2003). RhoA is required for cortical retraction and rigidity during mitotic cell rounding. *J. Cell Biol.* **160**, 255-265.

Mertins, P., Qiao, J. W., Patel, J., Udeshi, N. D., Clauser, K. R., Mani, D. R., Burgess, M. W., Gillette, M. A., Jaffe, J. D. and Carr, S. A. (2013). Integrated proteomic analysis of post-translational modifications by serial enrichment. *Nat. Methods* **10**, 634-637.

Ramachandran, C., Patil, R. V., Combrink, K., Sharif, N. A. and Srinivas, S. P. (2011). Rho-Rho kinase pathway in the actomyosin contraction and cell-matrix adhesion in immortalized human trabecular meshwork cells. *Mol. Vis.* **17**, 1877-1890.

Sebbagh, M., Hamelin, J., Bertoglio, J., Solary, E. and Bréard, J. (2005). Direct cleavage of ROCK II by granzyme B induces target cell membrane blebbing in a caspase-independent manner. *J. Exp. Med.* **201**, 465-471.

Seguin, L., Liot, C., Mzali, R., Harada, R., Siret, A., Nepveu, A. and Bertoglio, J. (2009). CUX1 and E2F1 regulate coordinated expression of the mitotic complex genes Ect2, MgcRacGAP, and MKLP1 in S phase. *Mol. Cell. Biol.* **29**, 570-581.

Su, L., Agati, J. M. and Parsons, S. J. (2003). p190RhoGAP is cell cycle regulated and affects cytokinesis. *J. Cell Biol.* **163**, 571-582.

Takizawa, C. G. and Morgan, D. O. (2000). Control of mitosis by changes in the subcellular location of cyclin-B1-Cdk1 and Cdc25C. *Curr. Opin. Cell Biol.* **12**, 658-665.

Tatsumoto, T., Xie, X., Blumenthal, R., Okamoto, I. and Miki, T. (1999). Human ECT2 is an exchange factor for Rho GTPases, phosphorylated in G2/M phases, and involved in cytokinesis. *J. Cell Biol.* **147**, 921-928.

Tripathi, B. K., Qian, X., Mertins, P., Wang, D., Papageorge, A. G., Carr, S. A. and Lowy, D. R. (2014). CDK5 is a major regulator of the tumor suppressor DLC1. *J. Cell Biol.* **207**, 627-642.

Wu, D., Asiedu, M., Adelstein, R. S. and Wei, Q. (2006). A novel guanine nucleotide exchange factor MyoGEF is required for cytokinesis. *Cell Cycle* **5**, 1234-1239.

Yaffe, M. B., Rittinger, K., Volinia, S., Caron, P. R., Aitken, A., Leffers, H., Gamblin, S. J., Smerdon, S. J. and Cantley, L. C. (1997). The structural basis for 14-3-3: phosphopeptide binding specificity. *Cell* **91**, 961-971.

Yoshizaki, H., Ohba, Y., Parrini, M.-C., Dulyaninova, N. G., Bresnick, A. R., Mochizuki, N. and Matsuda, M. (2004). Cell type-specific regulation of RhoA activity during cytokinesis. *J. Biol. Chem.* **279**, 44756-44762.

Zanin, E., Desai, A., Poser, I., Toyoda, Y., Andree, C., Moebius, C., Bickle, M., Conradt, B., Piekny, A. and Oegema, K. (2013). A conserved RhoGAP limits M phase contractility and coordinates with microtubule asters to confine RhoA during cytokinesis. *Dev. Cell* **26**, 496-510.